Crystalline Fibres of a Covalent Organic Framework through bottom1 up Microfluidic Synthesis †

David Rodríguezo Sano Miguel,[†a] Afshin Abrishamkar,[†b,c] Jorge A. R. Navarro,[d] Romen Rodriguezo Trujillo,[e] David B. Amabilino,[f] Ruben Maso Ballesté,*[a] Félix Zamora*[a,g,h] and Josep Puigmartío Luis*[b]

A microfluidic chip has been used to prepare fibres of a porous polymer with high structural order, setting a precedent for the generation of a wide variety of materials using this reagent mixing approach that provides unique materials not accessible easily through bulk processes. The reaction between 1,3,5o tris(4o aminophenyl)benzene and 1,3,5o benzenetricarbaldehyde in acetic acid under continuous microfluidic flow conditions leads to the formation of a higly crystalline and porous covalent organic framework (hereafter named as MFo COFo 1), consisting of fibrilar microo structures, which have a mechanical stability that allows for a direct drawing of objects on a surface.

Covalent organic frameworks (COFs) comprise an emerging class of molecular materials based on the atomically precise linking of organic subunits into two- or three-dimensional porous crystalline structures connected by covalent bonds with predictable control over composition, topology and porosity. [1-6,7] As a consequence of their inherent properties (e.g. low-density, porosity and crystallinity), COFs have been first explored for applications related to gas storage and separation.[1, 3, 5, 6, 8-12] Nevertheless, the suitable incorporation of new functional building blocks into their structure has paved the way to new potential uses as advanced materials, including application in catalysis, ultrasensitive sensing, optoelectronic applications, and clean energy technologies.[2, 4, 11, 13-17]

The majority of COFs synthesized to date are based on self-condensation reactions of boronic acids and/or their condensation with catechols.[18] These types of reactions require solvothermal reaction conditions (i.e. high operating temperatures) to form crystalline porous materials. On the other hand, although this type of COFs are typically thermally robust, they exhibit limited chemical stability, which strongly limits their use in many potential applications. In this context, the facile and dynamic nature of imine-bond formation in Schiff-base chemistry has blossomed, in the last few years for the synthesis of COFs.[19] The main reasons for this trend are their relatively high chemical stability, porosity and crystallinity in comparison to previously reported COFs.
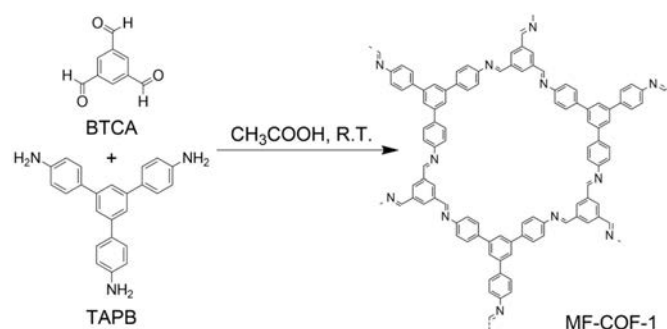
Scheme 1 Synthetic scheme of **MF-COF-1** at ambient conditions.

Even though these COFs are promising molecular materials for application in different areas, there is a need of protocols that facilitate their processability, and hence, enabling potential practical applications. Indeed processability of porous materials and, in particular metal-organic frameworks, is a subject of current reserach interest.[20, 21] In our quest for overcoming this drawback, we have recently published the fast synthesis, at room temperature, of a crystalline COF (**RT-COF-1**) resulting from the Schiff-base reaction between two trigonal building blocks, 1,3,5-tris(4-aminophenyl)benzene (TAPB) and 1,3,5-benzenetricarbaldehyde (BTCA).[22] As a result of the easy and rate tunable reaction, conducted under soft conditions, it was possible to perform direct on-surface patterning on rigid and flexible substrates by using both lithography-controlled wetting (LCW) and inkjet printing technologies.

a. Departamento de Química Inorgánica. Universidad Autónoma de Madrid. 28049 Madrid, Spain. E-mail: ruben.mas@uam.es; felix.zamora@uam.es.
b. Empa, Swiss Federal Laboratories for Materials Science and Technology, Lerchenfeldstrasse 5, 9014 St. Gallen, Switzerland. E-mail: josep.puigmarti@empa.ch
c. Department of Chemistry and Applied Biosciences, Institute for Chemical and Bioengineering, ETH Zurich, Vladimir Prelog Weg 1, 8093 Zurich, Switzerland.
d. Departamento de Química Inorgánica, Universidad de Granada, 18071 Granada, Spain.
e. Institut de Ciència de Materials de Barcelona (ICMAB-CSIC), Campus Universitari de Bellaterra, 08193 Cerdanyola del Vallès, Catalonia, Spain.
f. School of Chemistry, The University of Nottingham, University Park, NG7 2RD, United Kingdom.
g. Condensed Matter Physics Center (IFMAC). Universidad Autónoma de Madrid. 28049 Madrid, Spain.
h. Instituto Madrileño de Estudios Avanzados en Nanociencia (IMDEA Nanociencia), Cantoblanco, 28049 Madrid, Spain.
† These authors contributed equally to this work.
Electronic Supplementary Information (ESI) available: Additional experimental data. See DOI: 10.1039/x0xx00000x
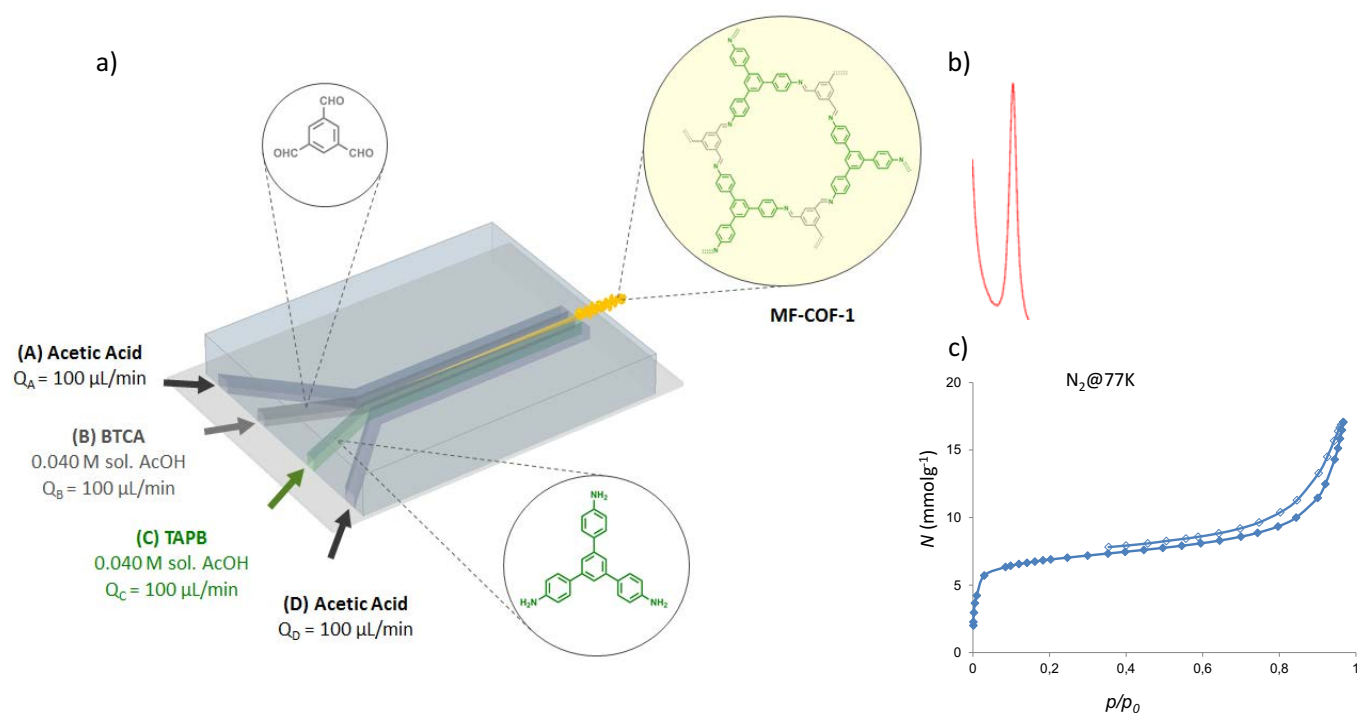
Fig. 1 a) Schematic representation of the microfluidic synthesis of **MF-COF-1**. b) X-ray powder diffractogram of **MF-COF-1**. c) N₂ isotherms at 77 K collected on **MF-COF-1**; filled dots: adsorption, empty dots: desorption.

Taking the flexibility of **RT-COF-1** processability a step further, and considering its fast and easy formation into crystalline form, here we report, for the first time, the synthesis of the imine-based COF material under continuous microfluidic conditions, hereafter named **MF-COF-1** (Scheme 1). Furthermore, we show how **MF-COF-1** can be produced in a few seconds (approx. 11 seconds), at atmospheric pressure and room temperature, in contrast to other COF processing technologies reported so far. In addition to that, we further demonstrate how microfluidic technologies can ease **MF-COF-1** direct printing in different orientations and complex forms on surfaces.

The microfluidic device used in this work is made of polydimethylsiloxane (PDMS) and is comprised of four input channels leading to a main microfluidic channel, where the reaction takes place (see ESI for further details). The main channel allows the reagents to slightly diffuse and react with each other under controlled diffusion conditions by varying the input flow rates of the reagent-laden flows ((B) and (C)) and the sheath flows ((A) and (D)), see Fig. 1a.[23] In a typical experiment, **MF-COF-1** was prepared using solutions of BTCA and TAPB in acetic acid (see ESI for further details). BTCA and TAPB solutions were injected, respectively, in (B) and (C) inlet channels while pure acetic acid was injected into channels (A) and (D). All solutions were injected into the microfluidic device through a syringe pump system and at flow rate 100 μL/min, i.e. a flow rate ratio (FRR) of 1 was used in our investigations. The microfluidic synthetic conditions were optimized to avoid the clogging of the main channel and to facilitate **MF-COF-1** direct printing on surfaces (see also movie S1 in the SI). Increasing the

FRR, which is defined as the ratio between the sheath flows and the reagent-laden flows, only changes the amount of **MF-COF-1** produced. That is, the amount of **MF-COF-1** produced decreases when increasing the FRR (see Fig. S7 in ESI). The role of acetic acid is crucial, since it catalyses both: i) the condensation reaction (resulting in a fast condensation process), and ii) the hydrolysis of imine groups; a result that allows for reversibility of the reaction and facilitates the formation of crystalline **MF-COF-1**. Thus, overall, by performing the reaction in pure acetic acid, a high degree of reversibility is achieved, resulting in dynamic chemical conditions that allow self-repair of adventitious defects during **MF-COF-1** formation. Recently, a microfluidic-based reactor was used to generate discrete molecular cages of a dynamic organic system based on imine condensation.[20] However, here we make use of the dynamic controlled over the mixing of reagents (BTCA and TAPB) to favour a greater degree of crystallinity of the resulting **MF-COF-1**.

Interestingly, the direct reaction between BTCA and TAPB, 1:1 molar ratio in acetic acid at room temperature under bulk chaotic mixing conditions leads to a characteristic viscous gel using regular synthetic conditions (**RT-COF-1Ac**). In contrast, microfluidic synthesis of **MF-COF-1** gives rise to the formation of jelly-like macroscopic fibres, which can be directly collected or deposited on surfaces.

The chemical and structural characterization of **MF-COF-1** are similar to those reported for **RT-COF-1,** which was obtained under ambient reaction conditions.[22] Indeed, a first spectroscopic assessment of the reaction product was made by

FT-IR spectroscopy (see Fig. S1 in ESI), which clearly shows the presence of imine C=N stretching band at 1623 cm^{-1} and the disappearance of amine N-H stretching bands in the 3500-3300 cm^{-1} region present in one of the starting materials. Solid state ^{13}C CP-MAS-NMR (see Fig. S2 in ESI) also confirmed the formation of the COF structure showing a signal at 156.7 ppm, corresponding to the iminic carbon atom. Elemental analysis is also consistent with the COF formation (see Table S1 in ESI). The analytical data corresponds to RT-COF-1 material with water (×0.75 molec.) and acetic acid (×1 molec.) molecules, which is a very common case for porous materials and especially for those containing basic sites, such as imines (ESI).
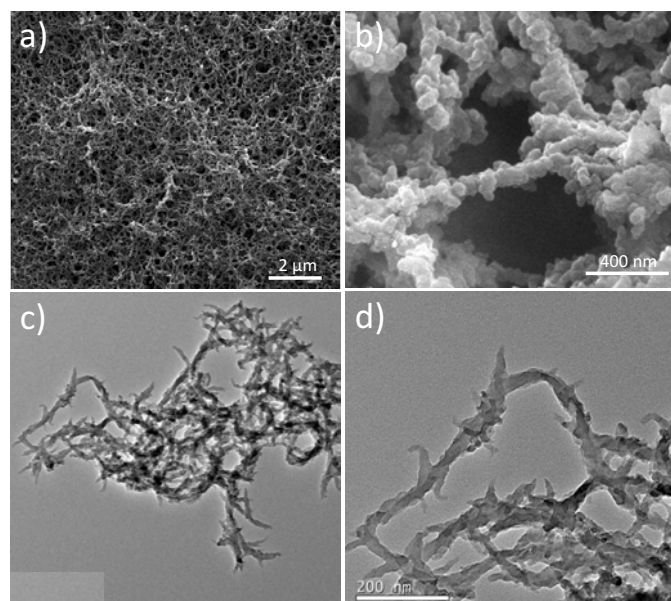

Fig. 2 a) and b) FESEM images and c) and d) TEM images of **MF-COF-1**.

An exceptional feature of **MF-COF-1** is its high crystallinity as proved by powder X-ray diffraction (Fig. 1b). Despite the short chip residence time experienced by the building blocks to perform the condensation reaction (approx. 11 seconds), the level of crystallinity is remarkable and even higher than **RT-COF-1**.[22] In particular, PXRD diffractograms of **MF-COF-1** show the most characteristic diffraction peaks of **RT-COF-1**, confirming its structure but with lower diffraction peak width indicating higher structural order for **MF-COF-1**. Similar features are also observed for **RT-COF-1Ac** (see Fig. S6 in ESI).

Once the **MF-COF-1** system was chemically and structurally characterised, we were also interested in knowing the possible effect of microfluidic synthesis on the material organization at the microscopic scale. With this purpose we have carried out scanning electron microscopy studies on **MF-COF-1** which show that the material is composed of meshes of fibres with *ca.* 70 nm diameter arranged in a macroporous sponge-like 3D branched structure (Fig. 2a). At higher magnification (Fig. 2b), it can be seen that these fibres are formed by 40 nm particles anisotropically aggregated in a linear fashion, probably due to the particular limited diffusion imposed by the flow conditions
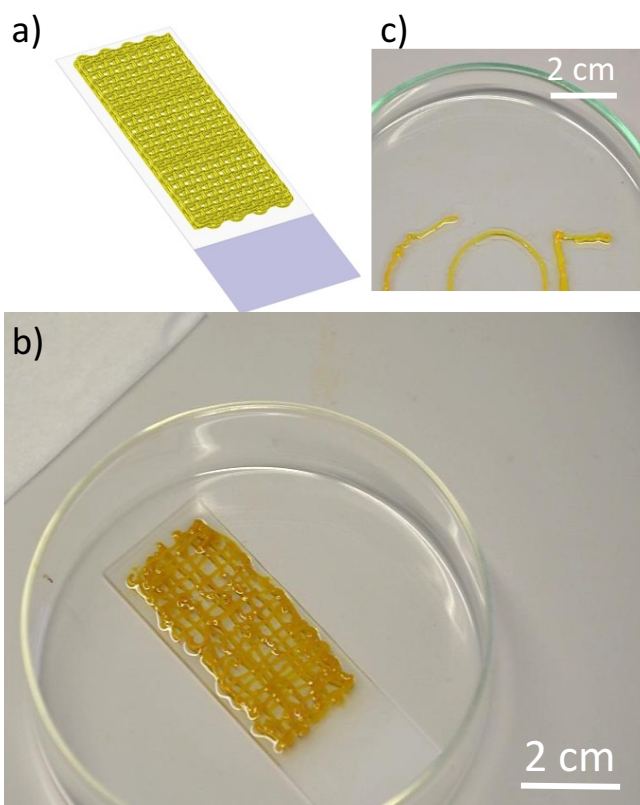

Fig. 3 a) Schematic illustration of the 3D **MF-COF-1** network printed in b) and in c) micrograph of a two-dimensional **MF-COF-1** structure on which was printed the word "COFs" on glass.

used during the microfluidic synthetic process. Note, that increasing the FRR does not change the fibrilar micro-structure of **MF-COF-1** (see Fig. S7 in ESI). Transmission electron microscopy (TEM) images of **MF-COF-1** also confirm the macroporous sponge-like morphology resulting from the interconnection of fibrous structures (Fig. 2c and 2d). Likewise, HR-TEM images are in agreement with the structure observed by SEM and suggest that the fibres and particles are not hollow. By contrast, FESEM images of **RT-COF-1Ac** also show aggregates of particles, but in this case of *ca.* 60 nm and not linearly organized (see Fig. S8 in ESI). In this case **RT-COF-1Ac** also exhibits a laminar morphology in some parts of the material. Therefore, we can conclude that electron microscopy images of **MF-COF-1** reveal unprecedented morphological features (Fig. 2a and 2b) when compared to other reported bulk COF samples[22] and **RT-COF-1Ac**.

Nitrogen isotherms were performed in order to confirm the accessibility of the porous structure of the **MF-COF-1** material to N$_2$ probe molecules at 77 K. For this purpose the material was thermally activated at 150 °C and a dynamic vacuum of 10^{-6} Torr was established prior to the measurement. The results show the formation of a type I isotherm typical of a microporous material with a BET and Lagmuir surface area values of 535 m^2 g^{-1} and 700 m^2 g^{-1}, respectively (Fig. 1c).[15, 24, 25] These values are slightly lower than those obtained for the material prepared in bulk under similar conditions, **RT-COF-1Ac** (Fig. S9). On the other hand, **MF-COF-1** material achieves a N$_2$ adsorption capacity of

ca. 8 mmol g-1 at the isotherm plateau (p/p_0= 0.5) which corresponds to a pore volume of *ca*. 0.28 cm^3/g. The notable increase of N$_2$ adsorption above p/p_0= 0.7 should be related to the macroporous sponge like organization of the material as visualized in the electron microscopy studies (see above).

Finally, an exciting capability of this synthetic approach is the possibility to employ the microfluidic chip described here as a printing tool to create complex two- or three-dimensional COF structures on surfaces, or eventually freestanding (see Fig. S10 in ESI). The yellow and flexible MF-COF-1 fibres coming out of the microfluidic chip can easily be adapted to various desired forms while being collected from the output channel (Fig. 3).

Conclusions

This work presents the first example of crystalline COF material generated under microfluidic conditions. Data presented herein demonstrates that the chemical composition and molecular structure obtained correspond to the expected 2D COF. However, microstructures observed by electron microscopy consist of interconnected fibres leading to 3D macroporous sponge-like organizations completely different to those formed under bulk chaotic mixing conditions. Therefore, it has been observed that the advanced mixing of reagents under microfluidic conditions allows a fine control over the formation of polymeric micro/nano-structures which facilitates the isolation of new nanoscaled forms inaccessible by any other technique. The mechanical properties of the as-prepared **MF-COF-1** fibres allow conformal 3D printing, thereby showing by this simple experiment the first conformal demonstration of a COF based material.

Furthermore, microfluidic-based synthesis of COFs open the door to a possible up scale production and their use on advanced patterning strategies such as 2D and 3D printing, envisaging a whole range of new technological applications.

Acknowledgements

Notes and references

1. A. P. Cote, A. I. Benin, N. W. Ockwig, M. O'Keeffe, A. J. Matzger and O. M. Yaghi, *Science*, 2005, **310**, 1166-1170.
2. S. Wan, J. Guo, J. Kim, H. Ihee and D. L. Jiang, *Angew. Chem. Int. Ed.*, 2008, **47**, 8826-8830.
3. R. W. Tilford, W. R. Gemmill, H. C. zur Loye and J. J. Lavigne, *Chem. Mater.*, 2006, **18**, 5296-5301.
4. E. L. Spitler and W. R. Dichtel, *Nat. Chem.*, 2010, **2**, 672-677.
5. R. W. Tilford, S. J. Mugavero, P. J. Pellechia and J. J. Lavigne, *Adv. Mater.*, 2008, **20**, 2741-2743.
6. H. M. El-Kaderi, J. R. Hunt, J. L. Mendoza-Cortes, A. P. Cote, R. E. Taylor, M. O'Keeffe and O. M. Yaghi, *Science*, 2007, **316**, 268-272.
7. J. X. Jiang and A. I. Cooper, *Top. Curr. Chem.*, 2010, **293**, 1-33.
8. A. P. Cote, H. M. El-Kaderi, H. Furukawa, J. R. Hunt and O. M. Yaghi, *J. Am. Chem. Soc.*, 2007, **129**, 12914-12915.
9. J. X. Jiang, F. Su, A. Trewin, C. D. Wood, H. Niu, J. T. A. Jones, Y. Z. Khimyak and A. I. Cooper, *J. Am. Chem. Soc.*, 2008, **130**, 7710-7720.
10. F. J. Uribe-Romo, J. R. Hunt, H. Furukawa, C. Klock, M. O'Keeffe and O. M. Yaghi, *J. Am. Chem. Soc.*, 2009, **131**, 4570-4572.
11. H. Furukawa and O. M. Yaghi, *J. Am. Chem. Soc.*, 2009, **131**, 8875-8883.
12. C. J. Doonan, D. J. Tranchemontagne, T. G. Glover, J. R. Hunt and O. M. Yaghi, *Nat. Chem.*, 2010, **2**, 235-238.
13. P. Kuhn, M. Antonietti and A. Thomas, *Angew. Chem. Int. Ed.*, 2008, **47**, 3450-3453.
14. E. L. Spitler, M. R. Giovino, S. L. White and W. R. Dichtel, *Chem. Sci.*, 2011, **2**, 1588-1593.
15. S. Y. Ding, J. Gao, Q. Wang, Y. Zhang, W. G. Song, C. Y. Su and W. Wang, *J. Am. Chem. Soc.*, 2011, **133**, 19816-19822.
16. X. S. Ding, J. Guo, X. A. Feng, Y. Honsho, J. D. Guo, S. Seki, P. Maitarad, A. Saeki, S. Nagase and D. L. Jiang, *Angew. Chem. Int. Ed.*, 2011, **50**, 1289-1293.
17. X. A. Feng, L. Chen, Y. P. Dong and D. L. Jiang, *Chem. Commun.*, 2011, **47**, 1979-1981.
18. S. Y. Ding and W. Wang, *Chem. Soc. Rev.*, 2013, **42**, 548-568.
19. J. W. Colson and W. R. Dichtel, *Nat. Chem.*, 2013, **5**, 453-465.
20. S. Furukawa, J. Reboul, S. Diring, K. Sumida and S. Kitagawa, *Chem. Soc. Rev.*, 2014, **43**, 5700-5734.
21. P. Falcaro, D. Buso, A. J. Hill and C. M. Doherty, *Adv. Mater.*, 2012, **24**, 3153-3168.
22. A. de la Peña Ruigómez, D. Rodríguez-San-Miguel, K. C. Stylianou, M. Cavallini, D. Gentili, F. Liscio, S. Milita, O. M. Roscioni, M. L. Ruiz-González, C. Carbonell, D. Maspoch, R. Mas-Ballesté, J. L. Segura and F. Zamora, *Chem. Eur. J.*, 2015, **21**, 10666-10670.
23. K. S. Elvira, X. C. I. Solvas, R. C. R. Wootton and A. J. deMello, *Nat. Chem.*, 2013, **5**, 905-915.
24. S. Kandambeth, A. Mallick, B. Lukose, M. V. Mane, T. Heine and R. Banerjee, *J. Am. Chem. Soc.*, 2012, **134**, 19524-19527.
25. P. Pachfule, M. K. Panda, S. Kandambeth, S. M. Shivaprasad, D. D. Diaz and R. Banerjee, *J. Mater. Chem. A*, 2014, **2**, 7944-7952.